Silicon (2024) 16:277–293
https://doi.org/10.1007/s12633-023-02663-5

RESEARCH

Study the Effect of Silicon Nanofluid on the Heat Transfer Enhancement of Triangular-Shaped Open Microchannel Heat Sinks

Mohammed Anees Sheik[1] · N. Beemkumar[1] · Arun Gupta[2] · Amandeep Gill[3] · Yuvarajan Devarajan[4] · Ravikumar Jayabal[4] · G. M. Lionus Leo[5]

Received: 21 May 2023 / Accepted: 3 September 2023 / Published online: 19 September 2023

Abstract
Comparative investigations were carried out for open and closed microchannel heat sinks for water and SiO2/water nanofluid, varying the Reynolds number from 200 to 800 and modifying the fin height from 0.5 mm to 2.0 mm. As part of its microchannel heat sink performance analysis, the study looked at several variables, including the Nusselt number, pressure drop, and cross-sectional fluid flow pattern and evaluated the optimum fin height. Nano SiO_2/water coolant enhances the Nusselt no. indicated that MCHS with 1.5 mm fin height has the most significant heat transfer value of 53.02. In contrast, MCHS with a 2.0 mm fin height has 38.68 using water as coolant. Water and nano SiO_2/water coolants had a maximum pressure drop of 187.90 and 286.96 Pa at 2.0 mm in height. The MCHS with 1.0 mm fin height has the maximum TPF of 2.17 and 1.75 for nano Sio_2/water and water as a coolant, respectively. TPF was increased by 24.19% and 46.24%, respectively, compared to water as a coolant and a closed microchannel heat sink in the triangular-shaped open MCHS with SiO_2/water nanofluid and 1.0 mm of fin height.

Keywords Sustainable energy · Renewable practices · Reliable energy · Clean energy · Energy efficiency

Nomenclature

ρ	Density (kg/m^3)
u, v	Velocity component (m/s)
k	Thermal conductivity (W/m ^{o}C)
D_h	Hydraulic diameter (m)
T	Temperature (^{o}C)
t	Time (s)
A	Area (m^2)
C_p	Specific heat (kJ/kg K)
h	Heat transfer coefficient (W/m^2 K)
P	Pressure (Pa)
q	Heat flux (W/m^2)
R_e	Reynolds number
N_u	Nusselt number

✉ N. Beemkumar
beem4u@gmail.com

✉ Yuvarajan Devarajan
dyuvarajan2@gmail.com

✉ Ravikumar Jayabal
raviram03@gmail.com

✉ G. M. Lionus Leo
lionusleo@gmail.com

[1] Departmen of Mechanical Engineering, Jain (Deemed to Be University), 560069, Bengaluru, Karnataka, India

[2] Department of Mechanical Engineering, Teerthanker Mahaveer University, Moradabad, Uttar Pradesh, India

[3] Department of R&D, Vivekananda Global University, Jaipur, Rajasthan, India

[4] Department of Mechanical Engineering, Saveetha School of Engineering, SIMATS, Chennai, Tamilnadu, India

[5] Department of Mechanical Engineering, St. Joseph's College of Engineering, Chennai, Tamil Nadu, India

1 Introduction

Over the past few decades, integrated circuit capabilities have improved so that billions of circuits may be manufactured on a single tiny chip. However, a more effective cooling system is required to keep the chip functioning since the heat flux is much greater. The microchannel heat sink (MCHS) heat transfer rate is higher than conventional heat exchangers, making the system more compact and less cumbersome. These benefits have led to the widespread use of MCHS in various industrial sectors. Traditional electronic devices often use fins and air as coolants for their microchips and microtubes. The quantity of heat produced by modern technology has increased over the years, but the poor thermal conductivity of air has made it harder for heat to dissipate. Therefore, liquid cooling is more efficient than air cooling in enhancing the thermal performance factor [1]. Geometrical elements such as the microchannel pattern, the number of inlets and outlets, the cross-section shape, nanofluids, and phase change materials influence the efficiency of the cooling process.

Tuckerman and Pease [2] initially used the term “microchannel cooling system” in 1981. Microchannel cooling is a passive way to eliminate heat from electronic devices that don’t take up as much space as other methods. An MCHS with a uniform geometrical layout is often used to efficiently remove heat from electronic components. As the capacity and use of microelectronic equipment have dramatically expanded, more heat is generated inside these devices. Smooth MCHS simply isn’t going to make it when dealing with such a high-temperature spike. Because of this, smooth MCHS needs enhancements to its thermal performance factor (TPF). Adding additional surfaces or cavities to the smooth channel may increase the TPF of the MCHS. TPF parameters such as Nusselt number and pressure drop will be compared between the modified and smooth channels. Several scientists are working toward increasing the heat dissipation rate with minimum pressure loss [3–6]. In the research, two significant strategies for heat transfer via single-phase coolant have mainly been used by adjusting channel design, which allows high heat disposal and increases coolant properties to transport more heat, such as dielectric, nanofluid, and refrigerant. Coolants, including oil, nanofluid, water, refrigerant, etc., have all been investigated. Although water is the most common coolant, nanofluids have recently gained popularity due to their ability to transport heat efficiently [7]. Nanofluids are filled with nanoparticles, which are small enough to pass through most materials. But nanofluid has several restrictions, such as sedimentation, higher pressure loss, and pipe wall abrasion from particle suspensions [8, 9]. Much work is being put in to address these concerns and ensure the safe usage of nanofluid in MCHS. Considerable expansion potential remains in this industry, especially for the coolant with outstanding heat transfer capacity, which is constantly preferred.

According to the research of Sui et al. [10], wavy rectangular microchannels have better thermal performance than straight baseline microchannels. The MCHS with rectangular, trapezoidal, and triangular cross sections were studied statistically by Wang et al. [11]. They found that trapezoidal microchannels had the highest thermal resistance, followed by triangular microchannels, out of the three possible MCHS geometries (rhombus, circular, and hexagonal). Hexagonal shapes, as shown by Alfaryjat et al. [12], are optimal for heat transfer. The most significant friction factor and heat resistance values were found in the rhombus cross-section. Deng et al. [13] investigated the properties of a copper microchannel with a form. Compared to traditional MCHS with a rectangular cross-section, the study indicated that the Nusselt number increased by 39% and heat resistance decreased by 22%. Other forms, such as those with cavities [14, 15], ribs [16, 17], and segmented fins [18, 19], have also been discussed in the literature. A microchannel’s surface roughness and shape affect heat transmission and fluid flow [20, 21]. Research has shown that surface roughness increases the pressure drop but has less effect on heat transmission.

Converging microchannels with very hydrophobic walls were studied by Ermagan and Rafee [22]. They noted that the highly hydrophobic walls enhanced TPF for pumping power. Pin fins with a staggered configuration in an MCHS were studied by Yang et al. [23] in five distinct shapes such as hexagon, square, pentagon, triangle, and circle. They conducted both numerical and experimental experiments with water and discovered that triangular pin fins had the most blocking effects, whereas circular pin fins had the least. The fin’s hexagonal cross-section provides the best heat conduction. Studies on oblique or segmented layouts of the fins demonstrate that additional flow paths improve fluid mixing, distort the thermal barrier layer, and redevelop it, leading to a higher heat transfer rate [24]. Sajedi et al. [25] conducted a numerical investigation of microchannels with both circular splitter plates. To minimize pressure, drop over the heat sink; splitter plates help drop the flow separation. Chein and Huang [26] studied electronic components’ functional behavior and reported that nanofluids have a more significant cooling impact.

The effects of Al2O3/water and SiO2/water nanofluids on TPF in a square cross-section cupric conduit were experimentally studied by Nassan et al. [27] under constant heat flux conditions. SiO2/water nanofluid was given a higher TPF than Al2O3/water nanofluid. The turbulent flow condition of Al2O3, TiO2, and SiO2 nanofluids at different ratios was studied by Rostamani et al. [28] in a 2D conduit. The particle ratio in volume was discovered to influence the TPF in nanofluids. Convective heat transfer through a circular tube with laminar flow and a constant wall temperature boundary condition was experimentally explored by Heris et al. [29]. The results showed that the heat transfer coefficient of SiO2 and Al2O3 nanofluids increases with both increasing the nanoparticle concentration and the Peclet number. Heris et al. [30] investigated the effects of SiO2, TiO2, and Al2O3 nanofluids in turbine oil on heat transmission using a circular tube. The performance index for every nanofluid under investigation was determined to be greater than one. They concluded that the nanofluid-based coolants were the most effective at transmitting heat. Pin fins and surface roughness were assessed for their respective importance by Sadaghiani and Kosar [31]. The heat transfer coefficient surrounding a fin in an MCHS was expected to be maximal near the wake's trailing edge downstream of the pin fin, which was confirmed by Wang et al. [32]. As the fin height varied, he discovered a heat sink configured openly with a fin height of 75% to 80% was more efficient at transferring heat than a heat sink configured closed. The author has outlined the advantages of an open MCHS [33].

Similarly, Yin et al. [34] reported that flow boiling instabilities might be significantly suppressed in the hollow microchannel, in addition to heat transmission improvements. In addition, Kadam et al. [35] demonstrated the advantages of an open MCHS over a closed MCHS. In addition, a summary of research done on the MCHS is provided in Table 1.

A significant research gap exists regarding exploring optimal fin height in MCHS, with limited studies conducted in this area. Additionally, there is a notable scarcity of research comparing the performance of open and closed MCHS configurations. In Open MCHS, the fin height is lower than the channel height allowing the fluid to flow between the fin top surface and the MCHS cover. As the fin height varies, the open space available above the fin height varies and vice versa. In Closed MCHS, the fin height equals the MCHS channel height, resulting in a fin top surface touching the MCHS cover. There has been little known work on fin design compared with open and closed MCHS.

Consequently, the proposed study aims to identify the heat transfer potential and overall performance of an open and closed MCHS consisting of a triangular fin. A comparative finding is performed by varying the open MCHS fin height from 0.5 mm, 1.0 mm, and 1.5 mm and the closed MCHS fin height of 2.0 mm. In addition, the optimal value of fin height that provides superior heat transfer and fluid flow characteristics has been determined by a thorough comparison of various heat sinks. An extensive comparative investigation is conducted by interchanging the fluid between water and nano SiO2/water as the fluid and varying the laminar flow Re from 200 to 800. Several factors, including fluid flow pattern, Nusselt number, and pressure drop, are considered while assessing the MCHS's performance. For this reason, the index for performance assessment criteria is developed and evaluated across all forms at different Reynolds numbers, such as the thermal performance factor.

2 Geometric Configuration

Figure 1 depicts the schematic representation of an MCHS. The reduced fine height demonstrates the open MCHS appearance that has formed in proportion to the channel height. The upper surface of the fin is thus separated from the heat sink surface by fluid. It's common knowledge that the shorter the fin, the more space below it, and likewise, in the other direction. The arrangement's coolant flows via the channel and the empty area. With this setup, the fins are submerged completely in the coolant, which frequently transfers heat to the fins' outer surface. Its circulation is distinct from that in a closed microchannel, which confines fluid to those specific routes. In this investigation, we use computational methods to examine the heat sinks' three-dimensional shape. As shown in Fig. 1, the physical dimensions of the computing domain are 27 mm in length, 10 mm in width, and 3 mm in height. The structure comprises a group of triangular pin fins of varied heights. The layout of the fins consists of four rows of 12 individual fins. Hence, there are 48 identical fins spaced out 1 mm from one another in a rectangular formation. As was previously indicated, the ideal configuration for the microchannel heat sink was discovered by varying the pin fin height. Almost every conceivable MCHS cross-section is considered, and the flow patterns on each cross-section and their impact on pressure drop and heat transfer at different Reynolds numbers are investigated.

3 Numerical Simulation

3.1 Governing Equations

The pressure loss and heat transfer in 3D geometry were simulated using ANSYS 2022 R1. The momentum equations regarding velocity and pressure have been solved using the SIMPLE Method Equation. To streamline our simulation models, we make a few assumptions. There was a laminar and incompressible steady-state flow condition, the influence of viscosity on heat dissipation and gravity was disregarded, and natural convection and radiation heat transfer were also disregarded. The governing equations are as follows, based on the assumptions above:

The energy equation for the liquid [31]

$$\rho_f C_{p_f} \frac{\partial T}{\partial t} + \rho_f C_{p_f} \left(\overrightarrow{U} \bullet \nabla T \right) = k_f \nabla^2 T \tag{1}$$

The energy equation for the solid [31]

$$\rho_s C_{p_s} \frac{\partial T}{\partial t} = k_s \nabla^2 T \tag{2}$$

Mass conservation equation [31]

$$\rho \nabla \bullet \left(\overrightarrow{U} \right) = 0 \tag{3}$$

Momentum equation [31]

Table 1 A summary of different MCHS

References	Study	Geometry type	Coolant fluid	MCHS Material	Remarks
[36]	Numerical	trefoil Shaped ribs	Water	Copper	Researchers observed that heat transmission and friction were enhanced when trefoil-shaped ribs were added to the walls of an MCSTR (Microchannel sidewall trefoil ribs), obtaining the most significant thermal enhancement factor, which became more prominent as Reynolds number increased
[37]	Numerical	Rectangular	Water hybrid nanofluid/Cu Al2O3	Copper	The findings demonstrate that the pressure drop is somewhat higher for hybrid nanofluids than for mono nanofluids, and the heat transfer rate rises as the nanoparticle volume percentage increases. The study also finds that hybrid nanofluids require less pumping power than Cu-water nanofluids
[38]	Numerical	Circular, rectangular, hexagonal, trapezoidal, elliptical, plus shape	Water	copper	The findings indicate that the suggested design of the novel plus-shaped microchannel has the potential to increase the cooling capabilities while minimizing the thermal resistance and entropy formation rate, resulting in improved energy efficiency
[39]	Numerical	Rectangle	Water	Copper	The research also showed that heat transfer accounts for more than 96% of the losses and that frictional losses may be disregarded at low Reynolds numbers. This study found that hydrofoil ribs performed better in hydrodynamic tests than elliptical ribs
[23]	Experimental and Numerical	Circle, square, triangle, pentagon, and hexagon	Water	Copper	It was observed that circular fins had the lowest pressure drop while hexagonal fins had the lowest heat resistance
[40]	Experimental and Numerical	Square, circular, triangular, Oval and diamond	Water	Copper	The friction coefficient was highest for circular pin fins and lowest for oval ones. A correlation formula between the Reynolds number and friction coefficient was developed using the experimental data
[41]	Numerical	Circular	Water	Silicon	The pumping powers medium and high, and the finned sink removes less heat than the best standard MCHS. At low pumping powers, finned heat sinks outperform basic MCHSs. Through entropy generation minimization, investigated heat sinks may be optimized
[42]	Numerical	Rectangular	Water	Copper	The research demonstrates entropy formation is significantly reduced when hot water is used for cooling, leading to improved 2nd law efficiency. This research may help develop more effective cooling methods for electrical equipment
[43]	Numerical	Wavy-wall	Water-copper nanofluid	Copper	Overall, the findings show how best to optimize heat transfer systems that use nanofluids in wavy channels

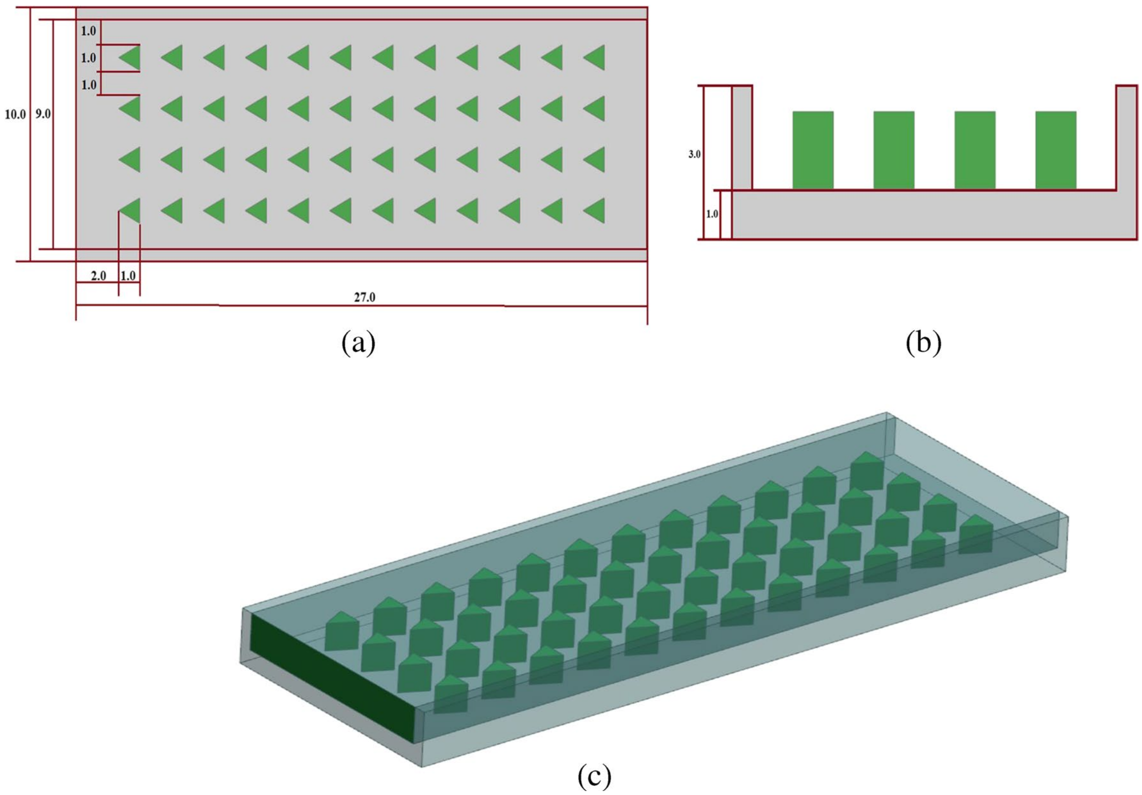

Fig. 1 Schematic representation of MCHS (**a**) Top view (**b**) Side view (**c**) Isometric view

$$\rho_f \frac{\partial \vec{U}}{\partial t} + \rho_f \left(\vec{U} \bullet \nabla \right) \vec{U} = -\nabla p + \mu \nabla^2 \vec{U} \tag{4}$$

4 Boundary Conditions

The heat sink material was considered copper, while the coolant was a water and nanofluid SiO2/water mixture of 0.15% of volume fraction. Table 2 depicts the material properties. The combined heat transfer solution is then employed to address the issue. The following are some of the steady-state assumptions made throughout this study: The fluid is incompressible and follows a Newtonian distribution; the flow is laminar and steady; and the adiabatic conditions and nonslip properties of the MCHS walls are preserved.

A SIMPLE method equation is incorporated into the simulation. For more precise simulation results, a second-order upwind method and set the convergence criterion to 10^{-6}. Figure 2 depicts the applied boundary condition in the domain of the numerical setup. All heat sinks and exterior walls are assumed adiabatic, and uniform heat flux was provided to their bottom surfaces. The no-slip boundary condition on the inside walls was considered, and the outlet boundary condition was adjusted to the atmospheric pressure outlet. The inlet velocity varies from 200, 400, 600 and 800 Re, and the heat flux input varies from 75,000, 100,000, 125,000, and 150,000 W/m2. The following equations show boundary conditions from Table 3.

5 Data Reduction

In an MCHS, several parameters are important for numerical calculations and evaluating its thermal performance. Here are some of the equations that have been used, such as the bulk temperature of the fluid, the average temperature of the MCHS wall, heat transfer coefficient, average Nusselt number, pressure drop, and thermal performance factor.

The fluid's bulk temperature refers to its average temperature as it enters or exits the microchannels. It represents the overall thermal behavior of the fluid in the heat sink. The bulk temperature is denoted by T_f and can be calculated using the following equation [36]:

Table 2 Thermophysical properties

Material	Viscosity (kg m^{-1} s^{-1})	Specific heat (kJ kg^{-1} K^{-1})	Density (kg m^{-3})	Thermal conductivity (W m^{-1} K^{-1})
SiO_2/water [44]	0.0015	4200	1030	0.78
SiO_2	–	381	8978	387.6
Water	0.001003	4182	998.2	0.6

$$T_{f\,x} = \frac{\int_{A_c} \rho u C_p T \, dA_C}{\int_{A_c} \rho u C_p \, dA_C} \tag{5}$$

The MCHS wall's average temperature represents the heat sink's thermal behavior. Tw denotes it and can be calculated using the following equation [36]:

$$T_{wx} = \frac{1}{w} \int_{w} T_w dw \tag{6}$$

The heat transfer coefficient (h_x) characterizes the heat transfer rate between the fluid and the MCHS wall. It is a measure of the effectiveness of heat transfer in the system. The heat transfer coefficient can be calculated using the following equation [23]:

$$h_x = \frac{q'' A_b}{(T_{w\,x} - T_{f\,x}) N A_i} \tag{7}$$

The average Nusselt number (N_u) is a dimensionless parameter that describes the convective heat transfer characteristics of the fluid in the microchannels. It is defined as the ratio of convective heat transfer to conductive heat transfer. The average Nusselt number can be calculated using the following equation [23]:

$$Nu_x = \frac{h_x D_h}{k_f} \tag{8}$$

$$Nu = \frac{1}{L} \int_{L} Nu_x dx \tag{9}$$

The pressure drop (ΔP) in the microchannels represents the resistance to fluid flow and is an important consideration in the design of microchannel heat sinks. It can be calculated using the following equation [23]:

$$\nabla P = P_{out} - P_{in} \tag{10}$$

The thermal performance factor (TPF) measures heat transfer efficiency in the microchannel heat sink. It can be defined as the ratio of the heat transfer rate to the pressure drop. The TPF can be calculated using the following equation [23]:

$$TPF = \frac{\frac{N_u}{N_{u_{plain}}}}{\left(\frac{\Delta P}{\Delta P_{plain}}\right)^{1/3}} \tag{11}$$

6 Mesh Independency

The grid independence is performed to determine the optimal mesh configuration. Six grids of hexahedral mesh were developed for the MCHS in this study to examine grid independence and verify the accuracy of numerical solutions. Independent meshes with element sizes of 0.3, 0.2, 0.15, 0.1, 0.09, and 0.0.8 mm were tested using a hexahedral mesh. The grid size detail concerning the number of mesh elements is depicted in Table 4. Pressure drop for the MCHS fin height of 1.5 mm was measured using water as a coolant to model the heat sinks' performance at a Reynolds number of 400. Figure 3 shows that the last three

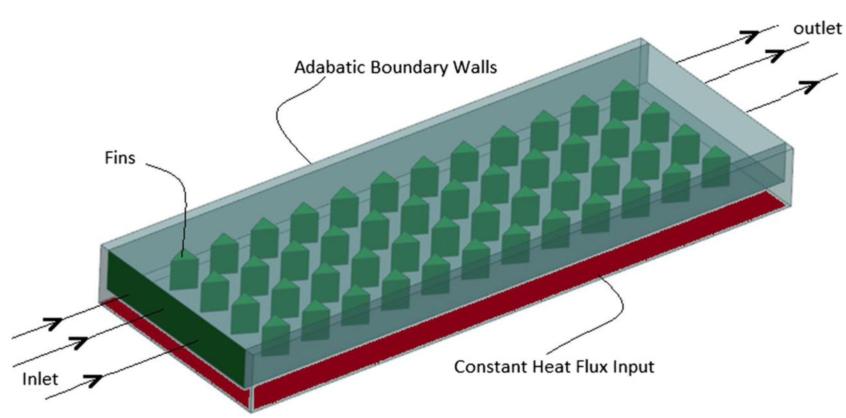

Fig. 2 Representing the numerical setup's domain's border conditions

Table 3 Boundary condition of MCHS

Surface	Boundary condition values	Boundary condition equations	Eq. No	Ref No
Bottom surface (Heat Flux in W/m2)	75,000, 100,000, 125,000, 150,000	$-k_a \frac{\partial T}{\partial y} = q$	(12)	[36]
Inlet (Velocity inlet in Re)	200, 400, 600, and 800	$u_x = u_{in}$ $u_y = u_z = 0$ $T = T_{in} = \text{const.}$	(13)	[36]
Outlet (Pressure outlet)	-	$\frac{\partial u_x}{\partial x} = \frac{\partial u_y}{\partial x} = \frac{\partial u_z}{\partial x} = 0$ $\frac{\partial T}{\partial x} = 0$	(14)	[36]
Interface	-	$u_x = u_y = u_z = 0$ $T_w = T_a$ $-k_w \frac{\partial T_w}{\partial n} = -k_a \frac{\partial T_a}{\partial n}$	(15)	[36]
Outer walls (Adiabatic condition)	-	$q = -k_a \frac{\partial T_a}{\partial n} = 0$	(16)	[36]

grids exhibit little difference in pressure drop results, such as 66.642, 66.844 and 66.957 Pa. The pressure drop deviation was determined to be between 2.91 to 0.1% by comparing data including 105,0674, 143,295, and 203,646, respectively, demonstrating that increasing the number of elements results in more reliable results. Hence, element 1050674 was chosen to represent this work because of its precision and low computational cost. Figure 4 depicts the meshing of the MCHS with a 1.5 mm fin height at a grid size of 0.1 mm.

7 Model Validation

Figure 5 depicts the Nusselt numbers for a plain microchannel heat sink at various Reynolds numbers, as reported by different references and the present work. The work shows relatively close agreement with Bhandari et al. [45]. At Reynolds numbers of 200 and 400, the present work and Bhandari et al. [45] have similar Nusselt number values, with a difference of only about 0.3–0.8, respectively. At Reynolds numbers of 600 and 800, the Nusselt number values from the present work are slightly higher than those from Bhandari et al. [45] but are still within a reasonable range.

On the other hand, the Nusselt number values reported by Yu et al. [46] and Shah and London [47] are higher than those from the present work. At Reynolds numbers of 200 and 400, the present work shows a difference of 0.5–2.5 and 1–2.1 from Yu et al. [46] and Shah and London [47], respectively. At Reynolds numbers of 600 and 800, the difference between the present work and the other two studies is even larger, with a difference of 2–3.5 and 1.3–2.6, respectively. The difference may be due to variations in the experimental setup, boundary conditions and measurement techniques used in the various studies. The outcomes of this investigation are in reasonable accord with those of other sources reporting outcomes for comparable Reynolds numbers. Comparing the current work's findings to those found in the literature helps to prove the validity and trustworthiness of the simulation setup used here.

8 Results

8.1 Heat Transfer Performance

In an MCHS, heat flux is an important parameter as it determines the rate of wasted heat from heat generating component. Several factors, including materials' thermal conductivity, rate of fluid flow, and geometry MCHS influence the heat flux. As the cooling fluid flows through the microchannels, it absorbs heat from the heat-generating component and carries it away from the heat sink. The effective heat flux from the bottom of MCHS to the contact wall area is depicted in Fig. 6. It can be observed that the effective heat flux values are lower than the heat flux values for all fin heights and heat flux levels. The reduction in effective heat flux is more significant for smaller fin heights than larger ones. The effective heat flux values decrease as the heat flux level increases, indicating a

Table 4 Details of mesh elements concerning grid size

Mesh Element size in mm	0.3	0.2	0.15	0.1	0.09	0.08
Number of mesh elements	55,680	166,705	360,408	1,050,674	1,432,995	2,036,446
Pressure Drop	56.901	61.457	64.745	66.642	66.844	66.957
Deviation (%)	–	8.00	5.35	2.91	0.303	0.169

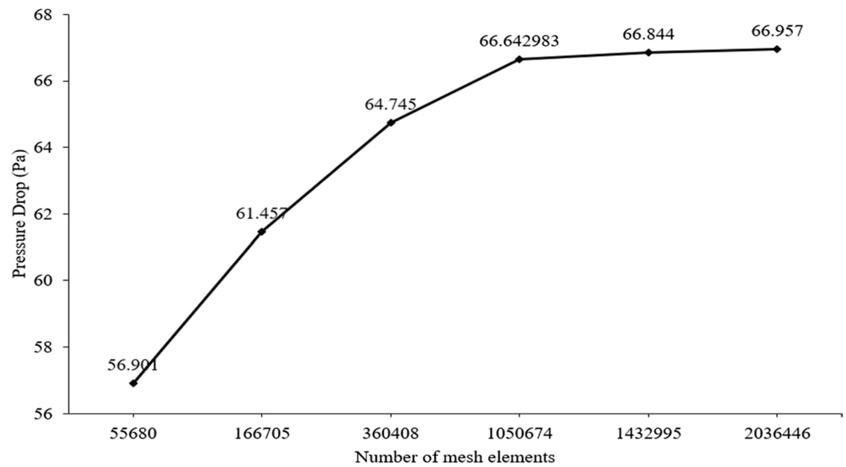

Fig. 3 Effect of mesh element size on pressure drop

reduced heat dissipation rate. The highest effective heat flux values are obtained for the largest fin height of 2 mm and the lowest heat flux rate of 75000W/m^2. Overall, Fig. 7 highlights the importance of effective heat flux in determining the thermal performance of MCHS.

Nusselt number is a quantitative measure of the convective heat transfer coefficient, which is a critical parameter in determining the overall performance of an MCHS. A higher Nusselt number leads to better heat transfer efficiency. This means an MCHS with a higher Nusselt number can dissipate more heat per unit area and achieve higher cooling performance. Higher Nusselt numbers may require higher pumping power or pressure drop, increasing energy consumption and decreasing overall system efficiency. Therefore, there is a trade-off between achieving higher Nusselt numbers and minimizing the energy consumption of the MCHS system.

Figure 7 shows that, as height increases, thermal resistance decreases, indicating better thermal performance of the MCHS. This is because higher fin heights provide more surface area for heat dissipation. Adding SiO2 nanoparticles to the water significantly improves the thermal performance of the MCHS at all fin heights and mass flow rates. Because of their excellent thermal conductivity, SiO2 nanoparticles speed up heat flow from the fluid to the fins. At low mass flow rates (200 and 400), the difference in thermal resistance between water and SiO2/water is relatively small. However, at higher mass flow rates (600 and 800), the benefits of using SiO2/water become more significant. The highest thermal resistance values are observed at the lowest fin height of 0.5 mm. This is because lower fin heights provide less surface area for heat dissipation, resulting in poorer thermal performance. The thermal resistance values decrease as the mass flow rate increases, indicating that higher flow rates result in better thermal performance. However, at very high flow rates, the benefits of increased flow rate may be offset by increased pressure drop and pumping power.

8.2 Fluid Flow Characteristics

Using SiO2/water as a coolant and a heat flux of 125,000, Figs. 8 and 9 show the velocity contour in the middle of the plain in the X & Y direction of the MCHS. The cross-sectional velocities increase as the fluid passes through the passage available between the MCHS fins. There is a decrease in velocity at the backside of steep angles of the fin cross-section, where the dead zones or areas of zero

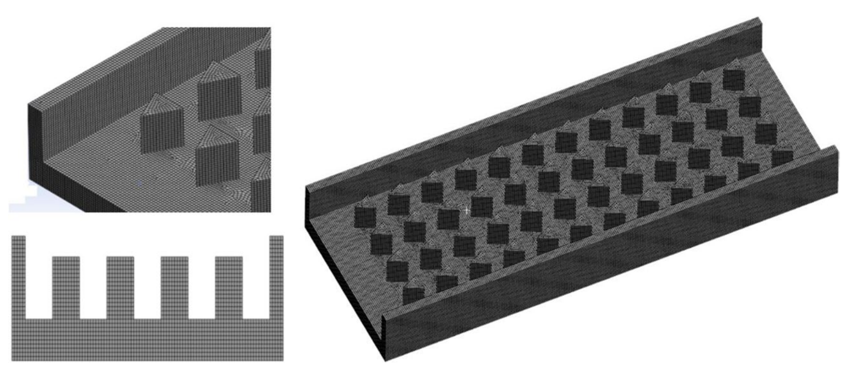

Fig. 4 Hexahedral meshing of MCHS for 1.5 mm of fin height

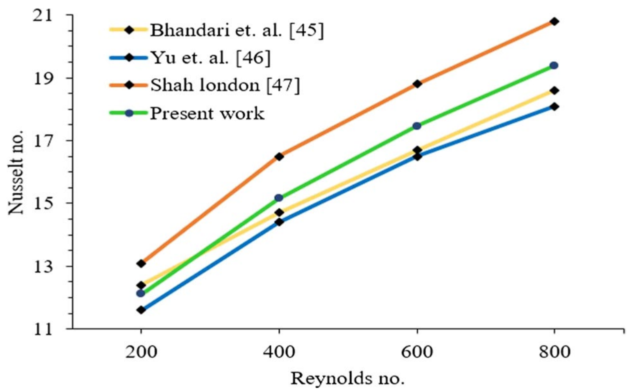

Fig. 5 Validation of the present work concerning Nu. and Re

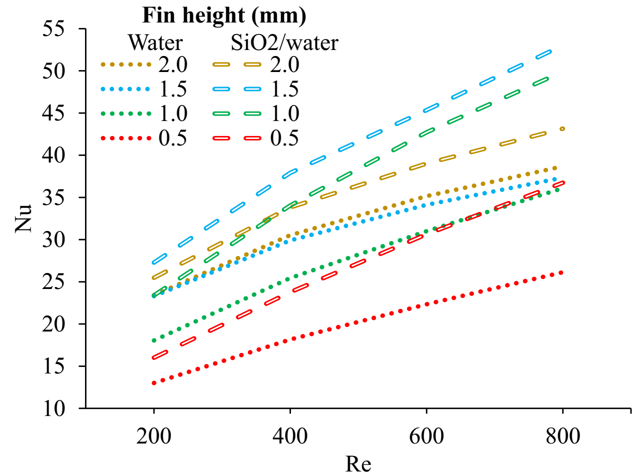

Fig. 7 Effective heat flux concerning different fin heights at different heat flux

velocity often occur. It can be observed for the cases or scenarios in the study. The heat transmission properties of MCHS are very sensitive to fluid flow patterns. Understanding the coolant flow stream, circulation, and interaction pattern across triangular pin fins requires understanding the coolant flow properties. A shear layer is generated when fluid flows over the fin of a pin because of the velocity difference between the fluid and the pin's fixed surface. Downstream of the fin, this shear layer generates vortices or eddies, which eventually merge into a wake, as shown in Fig. 10 at 600 Re and heat flux of 125000W/m2. The rear of the fins creates a wake or revolving vortices. Low velocities and high pressures in the wake zone cause to decrease in the heat transfer coefficient and an increase in thermal resistance.

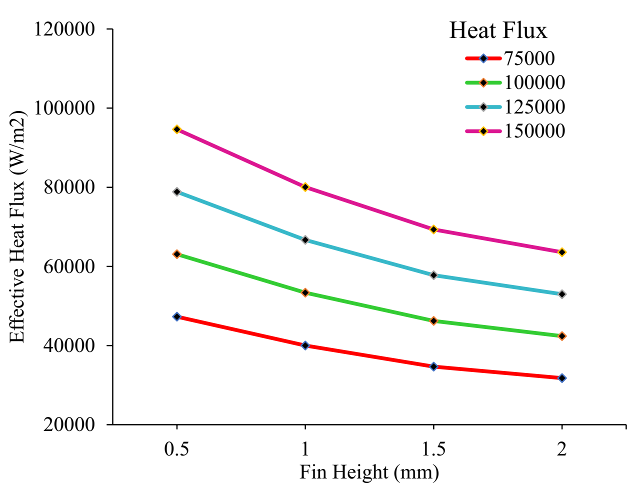

Fig. 6 Effective heat flux concerning different fin heights at different heat fluxes

8.3 Temperature Distributions

The temperature distribution in the working fluid is an important measure of thermal performance since it reveals where the heat is concentrated. The efficacy of MCHS is diminished by thermal maldistribution caused by high temperatures in localized areas. The heat transfer coefficient is enhanced due to the triangular pin fins' ability to expand the available heat transfer surface area and increase coolant turbulence. Employing triangular pin fins may influence the thermal boundary layer and heat transport properties. Inducing vortices in the coolant flow, like the triangle fins, may help with mixing and heat transmission. On the other hand, these vortices may lead to flow separation and decreased heat transmission in certain areas.

At a heat flow of 150000W/m^2, Fig. 11 depicts the contact wall temperature distribution across the MCHS at various fin heights at different Re. It can be observed that, with an increase in Re from 200 to 800, the contact wall temperature decreases. It is noticed that the highest decrease in contact wall temperature is at the fin height of 1.5 mm of open MCHS with nano SiO2/water as a coolant for the different Re. In the case of water as a coolant, it is observed that 2.0 mm of fin height of closed MCHS has the lowest contact wall temperature. The difference in temperature of open and closed MCHS, i.e., 1.5 mm fin height and 2.0 mm fin height using nano SiO2/water as a coolant for 200, 400, 600 and 800 Re, is 1.96, 1.82, 1.85 and 2.04, respectively. The reason for the drop in contact wall temperature of the open MCHS compared to closed MCHS is that increased available open space makes this feasible by increasing the net convective surface area responsible

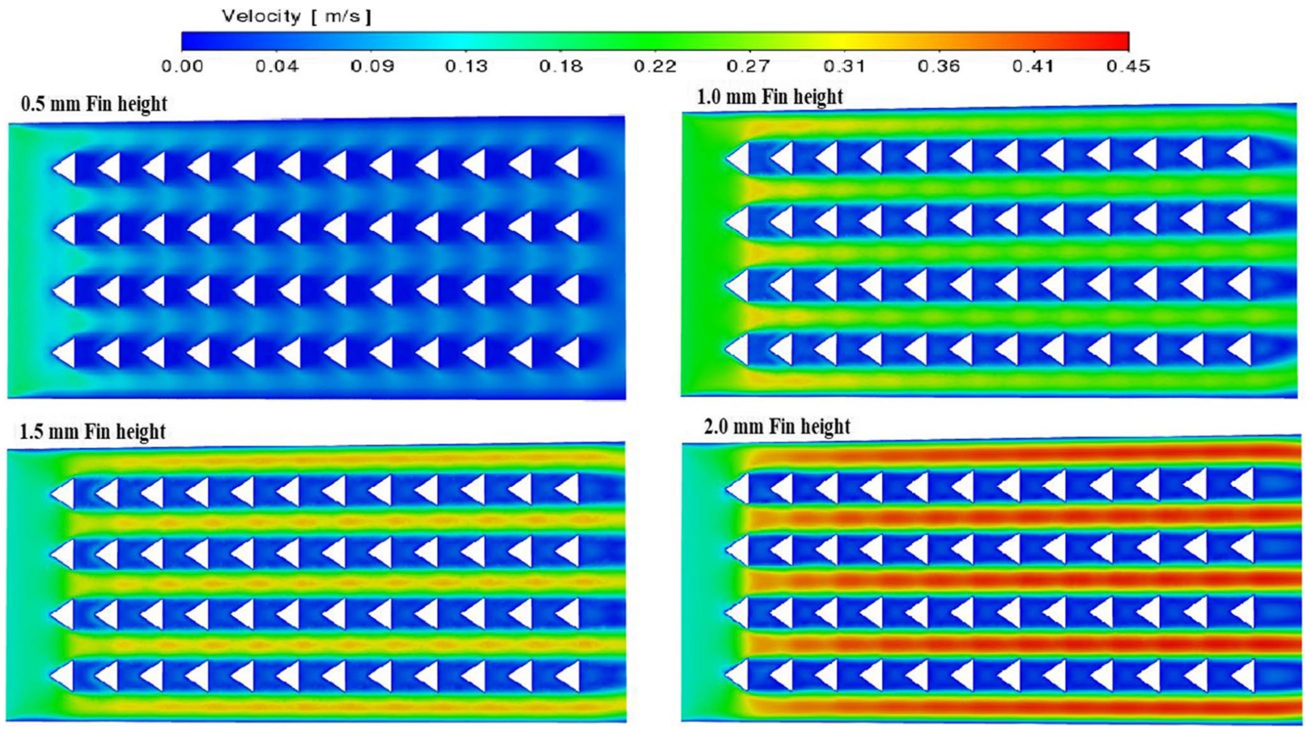

Fig. 8 Contour of velocity at the mid plain of fin height in X-direction at 125,000 heat flux and 600 Re. No. Using SiO2/water as a coolant

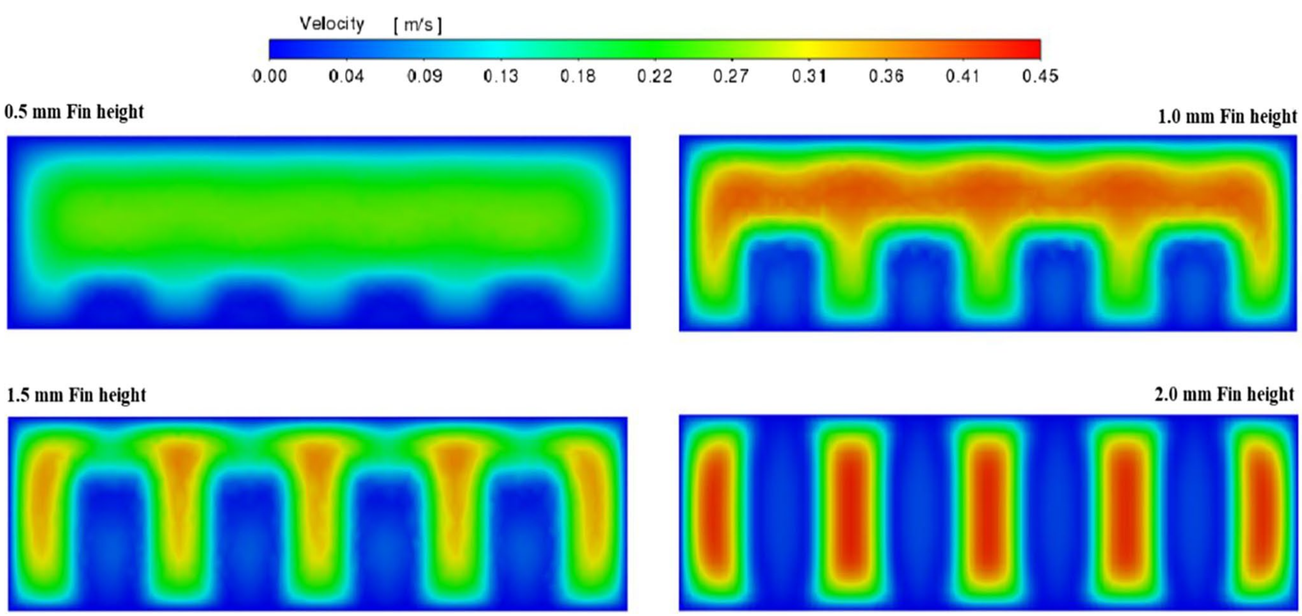

Fig. 9 Contour of velocity at the mid plain of the heat sink in Y-direction at 125,000 heat flux and 600 Re using SiO2/water as a coolant

for heat transfer, and it also allows for a more pronounced flow behavior of the coolant. Therefore, the thermal performance of a heat sink is determined by its convective surface area but also by the flow properties of the fluid within the heat sink.

At a Reynolds number of 800, Fig. 12 displays the temperature distribution of the various fin heights at the microchannel outlet. It can be observed that the contact wall temperature increases with an increase in heat flux input. Also, increased MCHS fin height leads to decreased contact wall

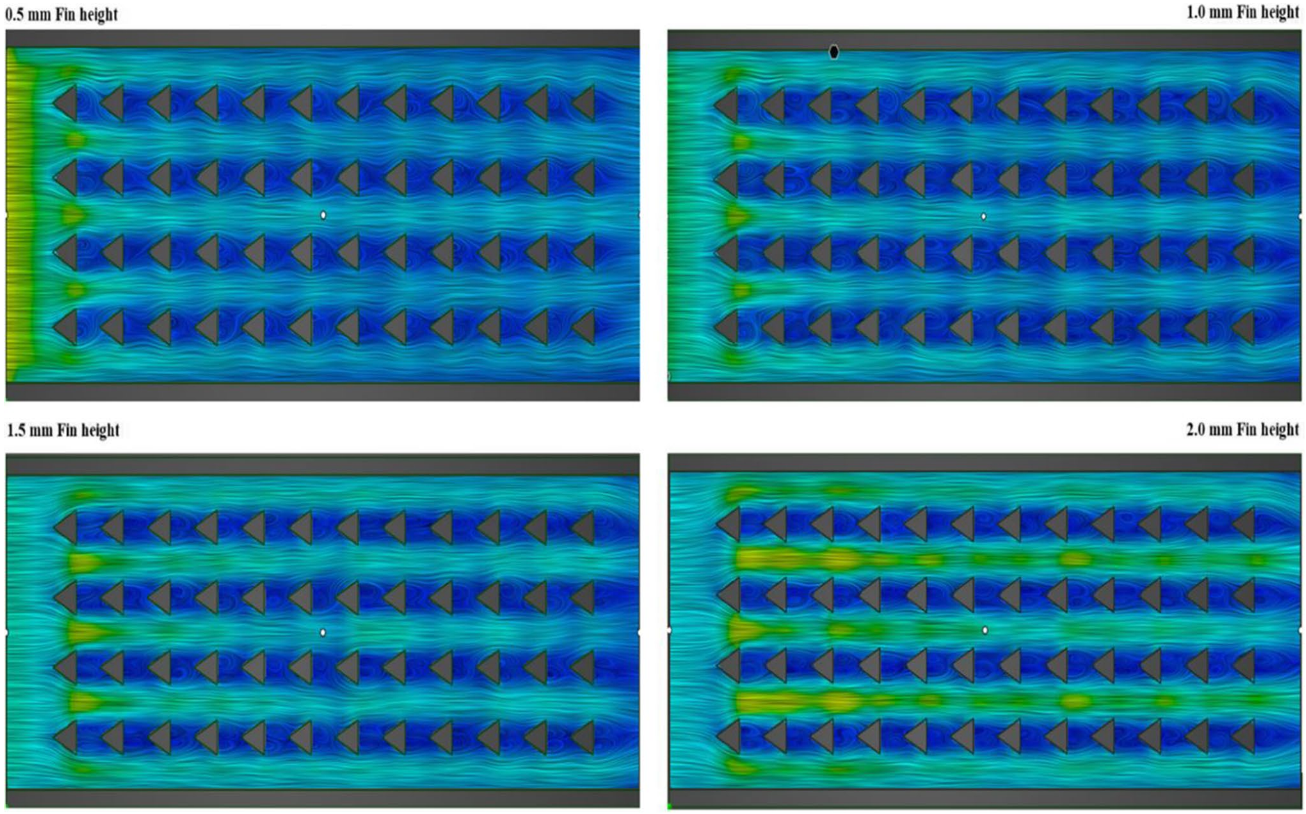

Fig. 10 Contour of velocity streamline and vortex generation of the heat sink at 125,000 heat flux and 600 Re, using SiO2/water as a coolant

temperature in the case of water as a coolant. Whereas in the case of nano SiO2/water, as a coolant contact wall temperature decreases with a rise in MCHS fin height from 0.5 mm to 1.0 mm and 1.0 mm to 1.5 mm, for the change in MCHS fin height from 1.5 mm to 2.0 mm, the contact wall temperature increases for all the heat flux input.

Figures 13 and 14 depicts the temperature contour at the bottom of the heat sink at 125,000 heat flux and 600 Re. No. They are using SiO2/water as a coolant. Typically, the temperature is higher near the inlet region of the microchannel heat sink due to the incoming hot fluid, which gradually decreases towards the outlet. The pin fins can cause localized temperature gradients, leading to hot and cold spots in the channel. The sharp edges of the triangular fins can induce vortices in the coolant flow, improving the mixing and heat transfer and decreasing temperature. Increasing the MCHS fin height results in a dramatic drop in temperature. It can be observed that the entrance fins towards the inlet are substantially cooler than the fins towards the outlet. The observed temperature in the wake zone, where the vertices are produced, is maintained at a somewhat lower temperature for 1.5 mm of MCHS fin height compared to 2.0 mm of MCHS fin height.

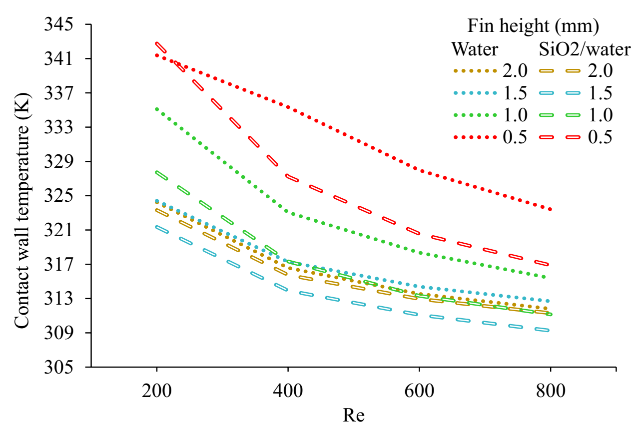

Fig. 11 Effective heat flux concerning different fin heights at different heat flux

8.4 Pressure Drop

Since the coolant flow rate is affected by pressure drop, the heat transfer rate and thermal performance of MCHS are also impacted. In MCHS, heat transfers efficiently because the channels are tiny yet have a high surface area to volume

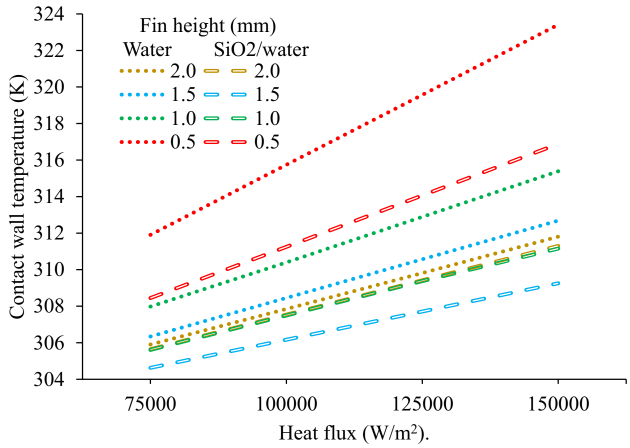

Fig. 12 Effective heat flux concerning different fin heights at different heat flux

ratio. However, compared to standard MCHS, this causes a greater pressure drop. Pressure drop, caused by frictional losses, often rises with flow rate. At high flow rates, the pressure drop may reach a critical value, beyond which flow instabilities can occur, resulting in reduced heat transfer efficiency and even flow reversal. The effects of pressure drop in MCHS can be significant. High-pressure drops can lead to increased pumping power and energy consumption, which can affect the overall efficiency of the cooling system. Also, high-pressure drops can result in uneven flow distribution among the channels, leading to hot spots and reduced cooling performance in certain heat sink regions. Therefore, it is important to carefully consider the pressure drop behavior and its effects in MCHS for optimal thermal management.

According to Fig. 15, the resistance to flow rises with a higher Reynolds number as the pressure drop increases for both water and SiO2/water fluid as the Reynolds number increases. It is seen that the SiO2/water fluid has a higher pressure drop than water at all Reynolds numbers, indicating that it is more viscous and, thus, harder to flow through the channel. For both fluids, increasing pressure drop increases with increasing fin height, suggesting that fin height is important in determining pressure drop. This might be because the fins provide greater resistance to air passage. The greatest pressure reductions are seen for water and SiO2/water fluids at a fin height of 2 and a Reynolds number of 800.

At Reynolds number 200, the pressure drop for water is between 8.86 to 31.66, while the pressure drop for SiO2/water is between 12.62 to 42.48. Similarly, at Reynolds number 800, the pressure drop for water is between 58.48 to 237.85, while for SiO2/water, it is between 77.03 to 286.96. However, it’s worth noting that the pressure drop for SiO2/water increases slower than for water as the Reynolds number increases. This could be due to nanoparticles in the SiO2/water mixture, which may alter the fluid flow and reduce turbulence. Overall, SiO2 nanoparticles in water

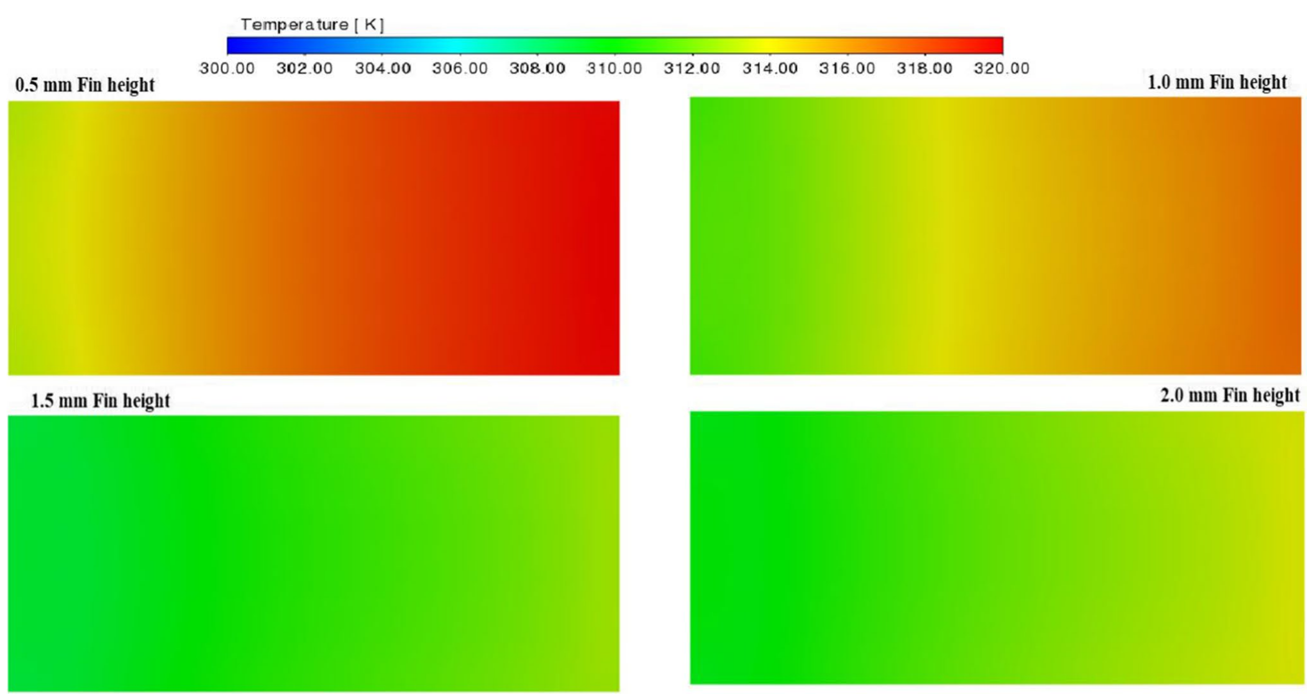

Fig. 13 Contour of temperature at the bottom of the heat sink at 125,000 heat flux and 600 Re. No. Using SiO2/water as a coolant

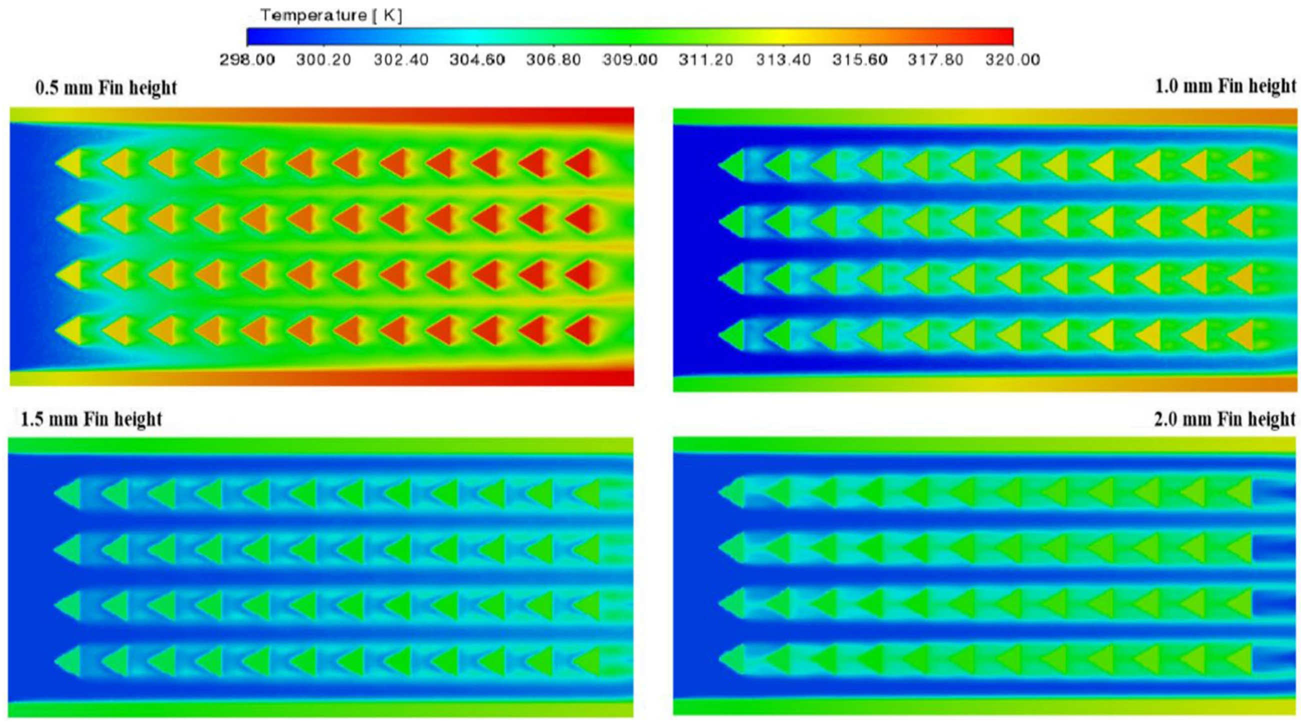

Fig. 14 Contour of temperature at the mid plain of the fin height at 125,000 heat flux and 600 Re. No. Using SiO2/water as a coolant

increase the flow resistance, leading to a higher pressure drop. Still, the effect is not significant enough to completely outweigh the potential benefits of using SiO2/water, such as improved thermal conductivity. Figure 16 depicts the pressure drop contour at the mid plain of fin height at 125,000 heat flux and 600 Re. No. Using SiO2/water as a coolant. It is easily observed that as the height of the fins increases, the pressure drop likewise increases and that the pressure continues to fall as the fluid moves along the channel between the fins and toward the outlet.

8.5 Performance Evaluation Criteria Index

The heat transfer rate and pressure drop are metrics used to assess MCHS's overall efficiency. The TPF evaluation criterion index provides a means of calculating their relative importance. Plain MCHS is the standard in commercial samples. All other forms were normalized. If the TPF for a given example is more than 1, then its performance is better than that of the baseline MCHS. The importance of TPF in MCHS design is that it provides a quantitative measure of the thermal efficiency of the heat sink. Higher TPF values indicate better heat transfer performance, which is desirable in applications where efficient heat dissipation is critical. By optimizing the TPF, MCHS can achieve better thermal performance while minimizing the pressure drop and fluid flow rate.

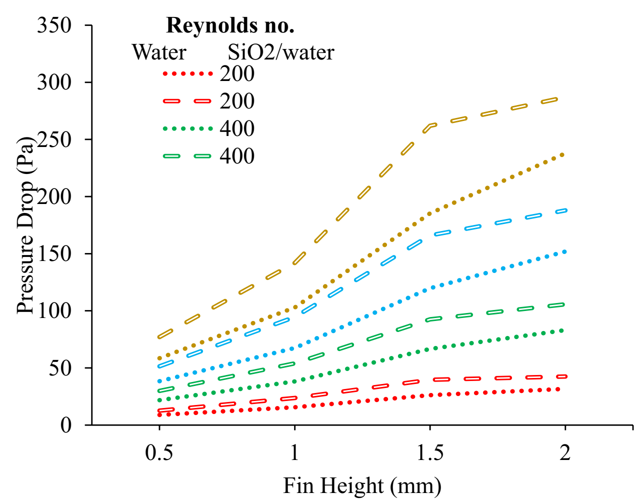

Fig. 15 Effective heat flux concerning different fin heights at different heat flux

Figure 17 depicts the TPF at different Reynolds numbers for different fin heights and coolants. It is seen that SiO2/water as a working fluid generally provides higher TPF values than water at all fin heights, indicating better heat transfer performance. At each fin height, the TPF values for SiO2/water are generally higher than those for water, indicating the superior thermal performance of SiO2/water. For a fin height of 1.0 mm with water coolant, the TPF values are

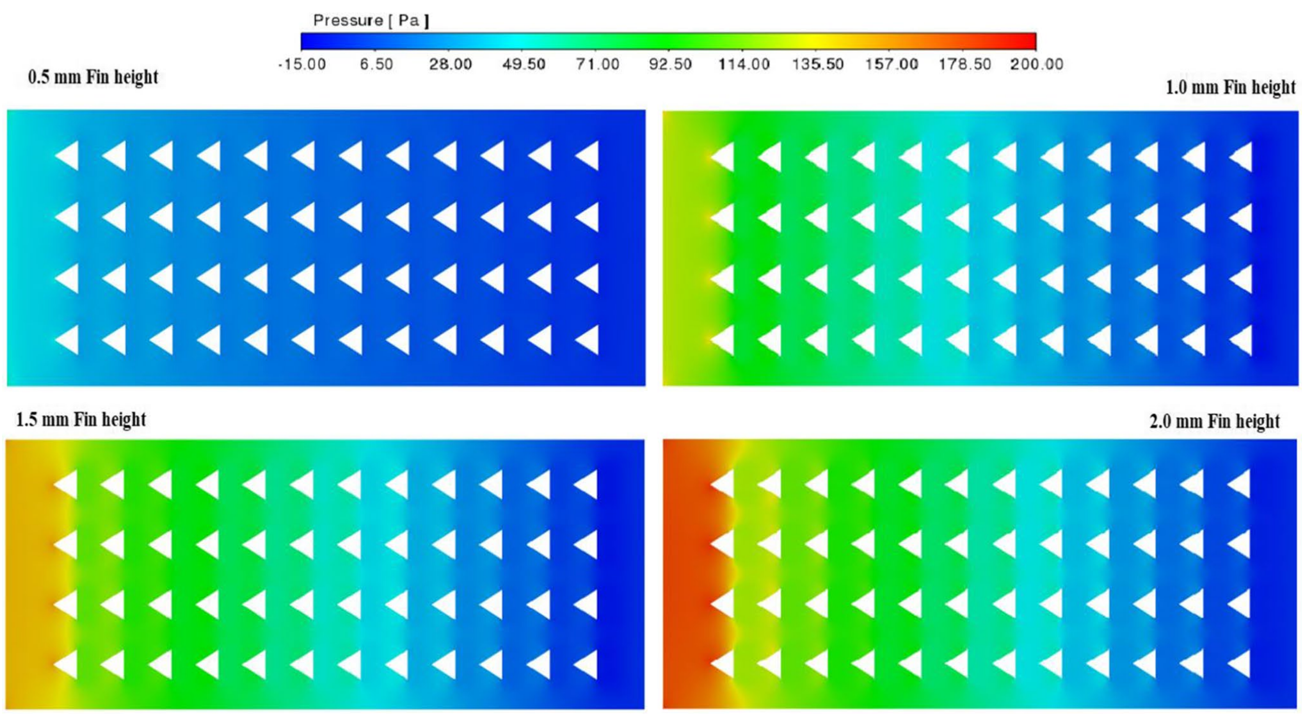

Fig. 16 Contour of pressure drop at the mid plain of fin height at 125,000 heat flux and 600 Re. No. Using SiO2/water as a coolant

consistently higher than for other fin heights, indicating that this is the most effective fin height for water as a coolant. Similarly, for a fin height of 1.0 mm with SiO2/water coolant, the TPF values are consistently higher than for other fin heights, indicating that this is the most effective fin height for SiO2/water coolant. It is observed that the difference in TPF of using water and nano SiO2/water as a coolant at a fin height of 1.0 mm is 0.198, 0.323, 0.4065, and 0.423 at 200. 400, 600 and 800 Re, respectively.

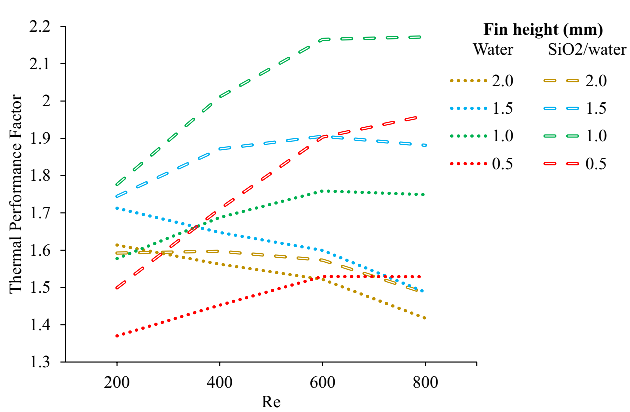

Fig. 17 TPF concerning Re at different fin heights

9 Conclusions

The present research provided a comprehensive analysis and comparison of open MCHS and closed MCHS with water and SiO2/water nanofluid as cooling fluids. The study focuses on the impact of varying fin height and Reynolds number on the heat transfer potential and overall thermal performance of the MCHS. The results highlight the effectiveness of SiO2 nanoparticles in improving thermal conductivity and heat transfer performance while also noting the potential drawbacks of increased pressure drop at higher flow rates.

- Optimal fin height was found to be crucial in maximizing both heat transmission and the characteristics of fluid flow.
- SiO2/water nanofluid showed better thermal performance than water at all fin heights and mass flow rates.
- SiO2/water increases the flow resistance, leading to a higher pressure drop. Still, the effect is not significant enough to completely outweigh the potential benefits of using SiO2/water, such as improved thermal conductivity and thermal performance factor.
- Heat transfer parameter Nusselt no. significantly increases by using nano SiO2/water as coolant. Results indicate that the MCHS with 1.5 mm of fin height provides the highest heat transfer with a maximum value of Nu is 53.02 nano SiO2/water as a coolant. In contrast,

water as a coolant in MCHS with 2.0 mm fin height provides the highest heat transfer value of Nu is 38.68.
- Pressure drop increased with increasing fin height for water and SiO2/water fluids. Results indicate maximum pressure drops of 187.90 and 286.96 Pa at the fin height of 2.0 mm for water and nano SiO2/water as a coolant, respectively.
- The MCHS with 1.0 mm fin height provides the highest TPF of about 2.17 and 1.75 for nano Sio2/water and water as a coolant. The results suggest that SiO2/water nanofluid is a promising coolant for MCHS, providing improved TPF by 0.42 compared to water at 1.0 mm of fin height.

The findings of this study can be used as a basis for designing and optimizing microchannel heat sinks for various applications, including electronic cooling and renewable energy systems.

10 Future Scope

The present study provides valuable insights into the thermal and flow characteristics of open MCHS and closed MCHS. However, several areas for future research could expand on this work, such as:

1. Investigating the effect of different nanoparticles and their concentrations on the thermal and flow characteristics of the MCHS.
2. Examining the impact of other parameters, such as fin thickness and spacing, on the performance of the MCSH.
3. Analysing the long-term reliability and durability of the heat sink under different operating conditions.
4. Exploring the application of the MCHS in other fields, such as electronics, renewable energy, and aerospace.
5. Developing optimisation techniques to determine the optimal combination of parameters for the MCHS design.

By addressing these future research directions, we can improve our understanding of the MCHS technology and enhance its performance and reliability in various applications.

Authors' Contributions Mohammed Anees Sheik and Beemkumar N Conceived the idea of the work and designed the experiments.

Arun Gupta, Amandeep Gill and G.M. Lionus Leo Performed the experiments and analysed the data.

Yuvarajan Devarajan & Ravikumar Jayapal supervised the study.

Data availability Not applicable.

Code Availability Not applicable.

Declarations

Ethics Approval Not applicable.

Consent to Participate Not applicable.

Consent for Publication Not applicable.

Competing interests The authors declare no competing interests.

References

1. Alihosseini Y et al (2021) Effect of liquid cooling on PCR performance with the parametric study of cross-section shapes of microchannels. Sci Reports 11(1):1–12. https://doi.org/10.1038/s41598-021-95446-0
2. Tuckerman D, R. P.-I. E. device letters, and undefined 1981, “High-performance heat sinking for VLSI,” *ieeexplore.ieee.org*, [Online]. Available: https://ieeexplore.ieee.org/abstract/document/1481851/. Accessed: Mar. 17, 2023
3. Sharma D, Pandey KM, Debbarma A, Choubey G (2017) Numerical Investigation of heat transfer enhancement of SiO2-water based nanofluids in Light water nuclear reactor. Mater Today Proc 4(9):10118–10122
4. Ajeel RK, Sopian K et al (2021) A Novel curved-corrugated channel model: Thermal-hydraulic performance and design parameters with nanofluid. Int Commun Heat Mass Transfer 120:105037. https://doi.org/10.1016/j.icheatmasstransfer.2020.105037. (**ISSN 0735-1933**)
5. Rehman MMU, Cheema TA, Ahmad F, Khan M, Abbas A (2019) Thermodynamic assessment of microchannel heat sinks with novel sidewall ribs. 34(2):243–254. https://doi.org/10.2514/1.T5770
6. Ali S et al (2021) Thermo-fluid characteristics of microchannel heat sink with multi-configuration NACA 2412 hydrofoil ribs. IEEE Access 9:128407–128416. https://doi.org/10.1109/ACCESS.2021.3109077
7. Chiu HC, Youh MJ, Hsieh RH, Jang JH, Kumar B (2023) Numerical investigation on the temperature uniformity of micro-pin-fin heat sinks with variable density arrangement. Case Stud Therm Eng 1(44):102853
8. Ajeel RK, Sopian K et al (2021) Thermal-hydraulic performance and design parameters in a curved-corrugated channel with L-shaped baffles and nanofluid. J Energy Storage 34:101996. https://doi.org/10.1016/j.est.2020.101996
9. Choubey G, Patel O, Solanki M, Ingenito A, Devarajan Y, Tripathi S (2023) Influence of cavity floor injection strategy on mixing improvement study of a splitter plate-assisted supersonic combustor. Eng Anal Bound Elem 155:995–1012
10. Sui Y, Lee PS, Teo CJ (2011) An experimental study of flow friction and heat transfer in wavy microchannels with rectangular cross section. Int J Therm Sci 50(12):2473–2482. https://doi.org/10.1016/J.IJTHERMALSCI.2011.06.017
11. Wang H, Chen Z, Gao J (2016) Influence of geometric parameters on flow and heat transfer performance of micro-channel heat sinks. Appl Therm Eng 107:870–879. https://doi.org/10.1016/J.APPLTHERMALENG.2016.07.039
12. Devarajan Y, Munuswamy D, Subbiah G, Mishra R (2023) Critical operating parameters of solar flat plate collectors using CuO

nanoparticles of different volume fractions subjected to natural convection. Environ Prog Sustain Energy:e14125
13. Deng D, Wan W, Tang Y, Shao H, Huang Y (2015) Experimental and numerical study of thermal enhancement in reentrant copper microchannels. Int J Heat Mass Transf 91:656–670. https://doi.org/10.1016/J.IJHEATMASSTRANSFER.2015.08.025
14. Ajeel RK, Zulkifli R et al (2021) "Numerical investigation of binary hybrid nanofluid in new configurations for curved-corrugated channel by thermal-hydraulic performance method. Powder Technol 385:144–159. https://doi.org/10.1016/j.powtec.2021.02.055
15. Bhandari P, Rawat KS, Prajapati YK, Padalia D, Ranakoti L, Singh T (2023) Design modifications in micro pin fin configuration of microchannel heat sink for single phase liquid flow: a review. J Energy Storage 30(66):107548
16. Li C, Li X, Huang H, Zheng Y (2023) Hydrothermal performance analysis of microchannel heat sink with embedded module with ribs and pin-fins. Appl Therm Eng 5(225):120167
17. Ajeel RK, Sopian K et al (2021) Assessment and analysis of binary hybrid nanofluid impact on new configurations for curved-corrugated channel. Powder Technol 32:3869–3884. https://doi.org/10.1016/j.apt.2021.08.041
18. Nagappan B, Devarajan Y, Kariappan E, Raja T, Thulasiram R (2023) A novel attempt to enhance the heat transfer rate of thermal energy storage using Multitemperature phase change materials through experimental and numerical modelling. Appl Therm Eng 227:120457
19. Ajeel RK, Salim WSIW (2019) Design characteristics of symmetrical semicircle-corrugated channel on heat transfer enhancement with nanofluid. Int J Mech Sci 151:236–250. https://doi.org/10.1016/j.ijmecsci.2018.11.022
20. Ajeel RK, Salim WS-I (2019) Turbulent convective heat transfer of silica oxide nanofluid through corrugated channels: an experimental and numerical study. Int J Heat Mass Transfer 145:118806. https://doi.org/10.1016/j.ijheatmasstransfer.2019.118806
21. Ajeel RK, Salim WS-IW (2019) Experimental and numerical investigations of convection heat transfer in corrugated channels using alumina nanofluid under a turbulent flow regime. Chem Eng Res Des 148:202–217. https://doi.org/10.1016/j.cherd.2019.06.003
22. Ajeel RK, Salim WS-IW, Hasnan K (2020) Numerical investigations of heat transfer enhancement in a house shaped-corrugated channel: Combination of nanofluid and geometrical parameters. Thermal Sci Eng Progress 17:100376. https://doi.org/10.1016/j.tsep.2019.100376
23. Bhandari P, Padalia D, Ranakoti L, Khargotra R, András K, Singh T (2023) Thermo-hydraulic investigation of open micro prism pin fin heat sink having varying prism sides. Alex Eng J 15(69):457–468
24. Bhore CV, Andhare AB, Padole PM, Loyte A, Vincent JS, Devarajan Y, Vellaiyan S (2023) Experimental investigation on minimizing degradation of solar energy generation for photovoltaic module by modified damping systems. Sol Energy 250:194–208
25. Ajeel RK, Salim WS-IW, Hasnan K (2019) Thermal performance comparison of various corrugated channels using nanofluid: numerical study. Alex Eng J 58(1):75–87. https://doi.org/10.1016/j.aej.2018.12.009
26. Chein R, G. H.-A. thermal engineering, and undefined 2005. Analysis of microchannel heat sink performance using nanofluids. Elsevier, [Online]. Available: https://www.sciencedirect.com/science/article/pii/S1359431105001006. Accessed: Mar. 18, 2023
27. Nassan T, Heris S, S. N.-I. C. in H. and, and undefined 2010. A comparison of experimental heat transfer characteristics for Al2O3/water and SiO2/water nanofluids in square cross-section duct. Elsevier. [Online]. Available: https://www.sciencedirect.com/science/article/pii/S0735193310000928. Accessed: Mar. 18, 2023
28. Ajeel RK, Saiful-Islam W, Sopian K, Yusoff MZ (2020) Analysis of thermal-hydraulic performance and flow structures of nanofluids across various corrugated channels: an experimental and numerical study. Therm Sci Eng Progress 19:100604. https://doi.org/10.1016/j.tsep.2020.100604
29. Heris S, Etemad S, M. E.-I. communications in heat, and undefined 2006, Experimental investigation of oxide nanofluids laminar flow convective heat transfer. Elsevier. [Online]. Available: https://www.sciencedirect.com/science/article/pii/S0735193306000194. Accessed: Mar. 18, 2023
30. Heris SZ, Farzin F, Sardarabadi H (2015) Experimental comparison among thermal characteristics of three metal oxide nanoparticles/turbine oil-based nanofluids under laminar flow regime. Int J Thermophys 36(4):760–782. https://doi.org/10.1007/S10765-015-1852-0
31. Yao Z, Derikvand M, Solari MS, Zhang J, Altalbawy FM, Al-Khafaji AH, Akbari OA, Toghraie D, Mohammed IM (2023) Numerical assessment of the impacts of non-Newtonian nanofluid and hydrophobic surfaces on conjugate heat transfer and irreversibility in a silicon microchannel heat-sink. J Taiwan Inst Chem Eng 1(142):104642
32. Beemkumar N, Yuvarajan D, Raja T, Selvarajan S (2023) Studies on enhancing the heat transfer rate of a multitemperature phase change materials-integrated thermal storage tank. Energy Sources A: Recovery Util Environ Eff 45(3):7578–7589. https://doi.org/10.1080/15567036.2023.2222682
33. Prajapati YK (2019) Influence of fin height on heat transfer and fluid flow characteristics of rectangular microchannel heat sink. Int J Heat Mass Transf 137:1041–1052. https://doi.org/10.1016/J.IJHEATMASSTRANSFER.2019.04.012
34. Yin L, Jiang P, Xu R, Hu H, Jia L (2019) Heat transfer and pressure drop characteristics of water flow boiling in open microchannels. Int J Heat Mass Transf 137:204–215. https://doi.org/10.1016/J.IJHEATMASSTRANSFER.2019.03.108
35. Kadam ST, Kumar R, Abiev R (2019) Performance augmentation of single-phase heat transfer in open-type microchannel heat sink 33(2):416–424. https://doi.org/10.2514/1.T5522
36. Ali S et al (2021) Numerical investigation of microchannel heat sink with trefoil shape ribs. Energies 14(20):6764. https://doi.org/10.3390/EN14206764
37. Krishna VM, Kumar MS, Muthalagu R, Kumar PS, Mounika R (2022) Numerical study of fluid flow and heat transfer for flow of Cu-Al2O3-water hybrid nanofluid in a microchannel heat sink. Mater Today Proc 49:1298–1302. https://doi.org/10.1016/J.MATPR.2021.06.385
38. Ahmad F, Ahmed F, Ali H, Rehman Z, Suleman M, Raouf I (2022) Effect of cross-sectional geometry on hydrothermal behavior of microchannel heat sink. J Non-Equilib Thermodyn 47(3):269–287. https://doi.org/10.1515/JNET-2021-0067/MACHINEREADABLECITATION/RIS
39. Ahmad F, Cheema TA, Khan A, Mohib-Ur-Rehman M, Yildizhan H (2021) Hydrothermal investigation of the performance of microchannel heat sink with ribs employed on side walls. J Non-Equilib Thermodyn 46(3):255–272. https://doi.org/10.1515/JNET-2020-0104/MACHINEREADABLECITATION/RIS
40. Munuswamy DB, Devarajan Y (2023) Critical examination of the role of silica nanoparticle dispersions in heat transfer fluid for solar applications. Silicon 15(1):571–581
41. Shafeie H, Abouali O, Jafarpur K, Ahmadi G (2013) Numerical study of heat transfer performance of single-phase heat sinks with micro pin-fin structures. Appl Therm Eng 58(1–2):68–76. https://doi.org/10.1016/J.APPLTHERMALENG.2013.04.008

42. Sharma CS, Tiwari MK, Michel B, Poulikakos D (2013) Thermofluidics and energetics of a manifold microchannel heat sink for electronics with recovered hot water as working fluid. Int J Heat Mass Transf 58(1–2):135–151. https://doi.org/10.1016/J.IJHEATMASSTRANSFER.2012.11.012
43. Ahmed MA, Shuaib NH, Yusoff MZ (2012) Numerical investigations on the heat transfer enhancement in a wavy channel using nanofluid. Int J Heat Mass Transf 55(21–22):5891–5898. https://doi.org/10.1016/J.IJHEATMASSTRANSFER.2012.05.086
44. Shukla KN, Solomon AB, Pillai BC, Ibrahim M (2012) Thermal performance of cylindrical heat pipe using nanofluids. 24(4):796–802. https://doi.org/10.2514/1.48749
45. Bhandari P, Prajapati YK (2021) Thermal performance of open microchannel heat sink with variable pin fin height. Int J Therm Sci 159:106609. https://doi.org/10.1016/J.IJTHERMALSCI.2020.106609
46. Yu X, Woodcock C, Plawsky J, Peles Y (2016) An investigation of convective heat transfer in microchannel with Piranha Pin Fin. Int J Heat Mass Transf 103:1125–1132. https://doi.org/10.1016/J.IJHEATMASSTRANSFER.2016.07.069
47. Shah R, London A (2014) Laminar flow forced convection in ducts: a source book for compact heat exchanger analytical data. Accessed: Mar. 22, 2023